

G.P. VASSILEV* , K.I. LILOVA**

CONTRIBUTION TO THE THERMODYNAMICS OF THE Co-Sn SYSTEM

WKŁAD W TERMODYNAMIKĘ UKŁADU FAZOWEGO Co-Sn

Comments on the available topological and thermochemical data of the Co-Sn system have been done. Updated data have been used in order to obtain adjustable coefficients for phase diagram calculation. In the present work both CoSn_3 modifications are modelled as different phases. The binary melt and the Co-based phases with face centred cubic and hexagonal structures are modelled as substitutional solutions. The allotropic forms of tin (αSn , βSn) as well as the intermediate phases CoSn , CoSn_2 , αCoSn_3 and βCoSn_3 are modelled as stoichiometric compounds. The phases $\alpha\text{Co}_2\text{Sn}_3$ and $\beta\text{Co}_2\text{Sn}_3$ are described by four sublattice model: $(\text{Co})_1(\text{Sn})_1(\text{Co},\text{Va})_{0.5}(\text{Co},\text{Va})_{0.5}$ in order to account for the order-disorder transition.

Reasonable agreement has been obtained between the calculated and the selected experimental thermodynamic and phase equilibrium data.

Keywords: lead-free solders; Co-Sn phase diagram; Thermodynamic optimization

W artykule dokonano przeglądu dostępnych danych topologicznych i termochemicznych dla układu Co-Sn. Uaktualnione dane wykorzystano w celu uzyskania współczynników dopasowania potrzebnych do obliczeń wykresu fazowego. W pracy obie odmiany CoSn_3 zostały zamodelowane jako różne fazy. Roztwór ciekły, oraz fazy na osnowie Co o strukturze sześcienniej ściennie centrowanej i heksagonalnej zamodelowano jako roztwory substytucyjne. Odmiany alotropowe cyny (αSn , βSn) a także fazy przejściowe CoSn , CoSn_2 , αCoSn_3 , βCoSn_3 potraktowano jako stechiometryczne związki. W celu uwzględnienia przemiany porządek- nieporządek fazy $\alpha\text{Co}_2\text{Sn}_3$ i $\beta\text{Co}_2\text{Sn}_3$ zostały opisane modelem czterech podsięci: $(\text{Co})_1(\text{Sn})_1(\text{Co},\text{Va})_{0.5}(\text{Co},\text{Va})_{0.5}$. Wyselekcjonowane dane eksperymentalne oraz obliczone wykazywały zadawalającą zgodność.

1. Introduction

It is anticipated that future lead-free solders would be based on tin-containing systems. Thus, the eutectic Sn-Co-Cu alloys have been suggested as prospective solders by Liu et al. [1]. Moreover, this work is part of a series of studies concerning prospective binary or ternary systems consisting of low melting metals (Zn, Sn, Bi, In) and elements of the Fourth or Fifth period (Ti, Ni, Co, Cu, Ag). Except for joining materials, as multicomponent solders or by the transient liquid phase bonding, such alloys could be applied in the galvanizing technologies or in specific for a system use. Particularly, some Co-Sn-Se phases would be interesting bearing in mind the optoelectronic and semiconductor properties of the binary cobalt- and tin-selenides [2–6].

The equilibrium phase diagram of the Co-Sn system is relatively well investigated [7–17]. The thermochemical properties of the binary liquid and solid alloys have

also been studied [18–22] but some discrepancies (concerning the liquid phase enthalpies of formation mainly) exist.

Previous thermodynamic assessments of this system are done by Ishida [23], Okamoto [24], by Jiang et al. [25], and by Liu et al. [26].

The equilibria between the liquid solution and the solid phases have been studied by Lewkonja [7], Zemczuzny and Belinsky [8], Hashimoto [9], and Darby and Juggle [10]. The latter authors worked in the tin-rich side, where the liquidus is very steep and the determination of the exact equilibrium concentration of the liquid phase is rather complicated.

Reading carefully the original works of Lewkonja [7], and Zemczuzny and Belinsky [8], we concluded that corrections of the temperatures, reported by these authors (and used as input data by Jiang et al. [25]), must be done. Actually, the melting point of the pure cobalt had been accepted to be 1440°C [7] and

* UNIVERSITY OF PLOVDIV, FACULTY OF CHEMISTRY, PLOVDIV, BULGARIA

** UNIVERSITY OF SOFIA, FACULTY OF CHEMISTRY, SOFIA, BULGARIA

1502°C [8], while presently established value is 1495°C (1768 K) [16]. The supposed Sn melting point had been, respectively, 232°C [7] and 231.5°C [8], while the contemporary value is 231.93 (505.1 K) [27].

Therefore, the purpose of the present work is to reconsider the topological and thermochemical data and to re-optimize the phase diagram Co-Sn using corrected (normalized) experimental values.

2. Thermodynamic optimization, results and discussion

The phase stabilities of the pure elements phases are those published by A. D i n s d a l e et al. [27, 28].

The solid solutions (α Co, ϵ Co) and the liquid phase have been modeled as disordered substitutional solutions in the above mentioned recent works [25, 26]. The concentration dependence of the excess G i b b s energy in such phases is described by R e d l i c h - K i s t e r polynomials, while the magnetic contribution to the G i b b s energy is calculated following an expression developed by H i l l e r t and J a r l [29].

The stoichiometric phases (Fig. 1) in the system are: CoSn, CoSn_2 , αCoSn_3 , βCoSn_3 , (α Sn) and (β Sn). Linear temperature dependences of their Gibbs energies of formation have been accepted for all of them, except for the βCoSn_3 , where one temperature independent term is used only. (α Sn) and (β Sn) are considered as identical with the corresponding pure substances.

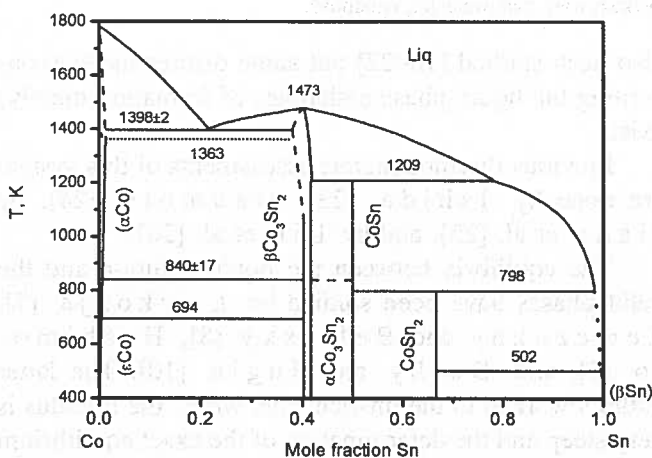
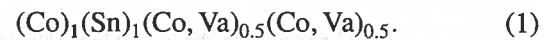


Fig. 1. Phase diagram of the system Co-Sn, up to M a s s a l s k i [16]. The dot line represents the Curie temperature

The compound Co_3Sn_2 is nonstoichiometric and exhibits two modifications. The high-temperature form ($\beta\text{Co}_3\text{Sn}_2$) is disordered (prototype $\text{Ni}_3\text{Sn}_2(\text{r})$), while long-range ordering exists in the low-temperature form ($\alpha\text{Co}_3\text{Sn}_2$, prototype $\text{NiAs}(\text{h})$ or B8_1) [30–32].

Waldner and Ipsier [33] have developed an approach to the thermodynamic modeling of $\text{B8}_{2(1)}$ -type compounds. In such a crystal lattice the tin atoms form a close-packed hexagonal sublattice, while the cobalt (1 and 2) atoms occupy the interstitial sites (e.g. Co(1) atoms fill all the octahedral interstitial sites, equal by number to the sites on the hexagonal sublattice; Co(2) atoms occupy part of the trigonal bipyramidal interstices of the Sn-atom array [30]). Due to the narrow $\beta\text{Co}_3\text{Sn}_2$ homogeneity range and in agreement with the chemical composition, the occupancy of the latter sites must be around $50\pm 6\%$. Consequently, four-sublattice model is needed in order to account for the order-disorder transformation, as discussed in details previously [33, 34]:



Such an approach has been applied by J i a n g et al. [25] while L i u et al. [26] have modeled this phase as stoichiometric compound. Besides, one should be aware that the input information used in the present work (Table 1) is different from that one of J i a n g et al. [25], because corrections of the experimental liquidus temperatures have been introduced by us, as mentioned.

In support of the normalization we would like to notice that after temperature corrections, the high-temperature eutectic invariant (Table 2) is estimated to lie at 1414 ± 7 K (by statistics of the normalized data of L e w k o n j a [7]). This is in good agreement with the recent measurements of C ö m e r t and P r a t t [14] giving a value of 1398 ± 2 K. Similarly, good accord between both authors is observed for the peritectic temperature P1 (1239 K) as well (Table 2).

The ferromagnetic transition in the cobalt-tin face centered cubic (FCC) solid solutions has been studied by H a s h i m o t o [9] who found that tin additions diminish the temperature of the magnetic ordering. C ö m e r t and P r a t t [14] contributed largely to the determination of the solvus. Low tin solubility (around 1 at. % Sn) in the FCC cobalt has been found, while such a data is missing for the hexagonal cobalt. In the latter, however, even inferior solubility is expected, like in the Co-Zn system [35], for example.

The precise cobalt solubility in the solid tin (α Sn) or (β Sn) is unknown, but it is anticipated to be negligible. Such a behavior is in agreement with theoretical considerations, taking into account that both, size- and electronegativity- factors are unfavorable (the metallic radii differ by about 25% ($r_{\text{Co}} = 125.2$ pm and $r_{\text{Sn}} = 162.3$ pm [36]), while Co and Sn atoms exhibit similar P a u l i n g electronegativities (1.88 for Co and 1.96 for Sn) [37]).

TABLE 1

Experimental information used for the assessment of the Co-Sn system

Type of the data	Reference
Topological data for the liquidus and the invariants (normalized temperatures)	[7]
Topological data for the liquidus and the invariants (normalized temperatures)	[8]
Topological data for the liquidus and the invariants	[9]
Topological data for the liquidus	[10]
Activities of tin in the solid phases (1273, 1073, 773 K) and extrapolated activities in the liquid phase (1273, 1073);	[12]
Topological data about the phase boundaries.	
Topological data about the phase boundaries and the invariants.	[14]
Temperature of the Congruent melting point of Co_3Sn_2 .	
Temperature of the order-disorder transformation in Co_3Sn_2 .	
Thermochemical data about the melting temperature of CoSn_2 and CoSn_3	[17]
Enthalpy of formation of liquid alloys (1823, 1780, 1759, 1675, 1671 K)	[19]
Enthalpy of formation of CoSn , Co_3Sn_2	[20]
Enthalpy of formation of CoSn	[21]

TABLE 2

Temperatures, types and notations of the invariant equilibria in the Co-Sn system. X_i – calculated compositions (tin mol fractions) of the coexisting phases; C.M. – congruent melting; PD1 – hypothetical peritectoid reaction; ED1 – hypothetical eutectoid reaction; P4 – degenerated peritectic reaction; ED2 – degenerated eutectoid reaction; PD2 and PD3 – degenerated peritectoid (eutectoid) reactions

Invariant reaction	Type	Temperature, K	Source
$L \leftrightarrow (\alpha\text{Co}) + \beta\text{Co}_3\text{Sn}_2$ $X_L = 0.230$; $X_{\text{FCC}} = 0.016$; $X_{\beta\text{Co}_3\text{Sn}_2} = 0.393$	Eutectic (E1)	1414 ^A 1378 ^A 1381 1398 ± 3 ~1385 1376 1381 1400	[7] [8] [9] [14] [23] ^E [25] ^E [26] ^E this work ^E
$L \leftrightarrow \beta\text{Co}_3\text{Sn}_2$ $X_L = X_{\beta\text{Co}_3\text{Sn}_2} = 0.399$	(C.M.)	1473 1443 1454 1472 1472	[14] [23] ^E [25] ^E [26] ^E this work
$L + \beta\text{Co}_3\text{Sn}_2 \leftrightarrow \text{CoSn}$ $X_L = 0.729$; $X_{\beta\text{Co}_3\text{Sn}_2} = 0.418$; $X_{\text{CoSn}} = 0.500$	Peritectic (P1)	1239 ^A 1196 ^A 1239±3 1209 1238 1216 1240	[7] [8] [14] [23] ^E [25] ^E [26] ^E this work
$\beta\text{Co}_3\text{Sn}_2 \leftrightarrow \alpha\text{Co}_3\text{Sn}_2$ unidentified compositions $\alpha\text{Co}_3\text{Sn}_2 \leftrightarrow \beta\text{Co}_3\text{Sn}_2 + (\alpha\text{Co})$ $X_{\alpha\text{Co}_3\text{Sn}_2} = 0.397$; $X_{\beta\text{Co}_3\text{Sn}_2} = 0.406$; $X_{\text{FCC}} = 8.3\text{E-}4$ $\beta\text{Co}_3\text{Sn}_2 \leftrightarrow \alpha\text{Co}_3\text{Sn}_2 + \text{CoSn}$ $X_{\beta\text{Co}_3\text{Sn}_2} = 0.411$; $X_{\alpha\text{Co}_3\text{Sn}_2} = 0.399$; $X_{\text{CoSn}} = 0.5$	Order/disorder transformation and related invariants (PD1) ^B (ED1) ^B	840±17 840 826 793	[14] [26] ^E this work this work
$L + \text{CoSn} \leftrightarrow \text{CoSn}_2$ $X_L = 0.959$; $X_{\text{CoSn}} = 0.500$; $X_{\text{CoSn}_2} = 0.6667$	Peritectic (P2)	819 ^A 787 ^A 823 844±3 798 843 798 845	[7] [8] [14] [17] [23] ^E [25] ^E [26] ^E this work

Table 2. (continuation)

Invariant reaction	Type	Temperature, K	Source
$(\alpha\text{Co}) \leftrightarrow (\epsilon\text{Co}) + \alpha\text{Co}_3\text{Sn}_2$ $X_{\text{FCC}} = 2.8\text{E-}4; X_{\text{HCP}} = 3.5\text{E-}5; X_{\alpha\text{Co}_3\text{Sn}_2} = 0.397$	Eutectoid (ED2) ^C	694 ~693 695 696 693	[14] [23] ^E [25] ^E [26] ^E this work
$\text{L} + \text{CoSn}_2 \leftrightarrow \beta\text{CoSn}_3$ $X_{\text{L}} = 0.996; X_{\text{CoSn}_2} = 0.6667; X_{\beta\text{CoSn}_3} = 0.75$	Peritectic (P3)	618±2(DSC) 623±5(DTA) 618	[17] [17] this work
$\beta\text{CoSn}_3 \leftrightarrow \alpha\text{CoSn}_3$ $X_{\beta\text{CoSn}_3} = 0.75; X_{\alpha\text{CoSn}_3} = 0.75$ $\beta\text{CoSn}_3 \leftrightarrow \alpha\text{CoSn}_3 + \text{L}$ $X_{\beta\text{CoSn}_3} = 0.75; X_{\alpha\text{CoSn}_3} = 0.75; X_{\text{L}} = 0.999$ $\beta\text{CoSn}_3 \leftrightarrow \alpha\text{CoSn}_3 + \text{CoSn}$ $X_{\beta\text{CoSn}_3} = 0.75; X_{\alpha\text{CoSn}_3} = 0.75; X_{\text{CoSn}} = 0.5$	Polimorphic transformation and related invariants (P4) ^C (PD2) ^C	548±5 548 548	[17] this work this work
$\text{L} \leftrightarrow \alpha\text{CoSn}_3 + (\beta\text{Sn})$ $X_{\text{L}} \approx 1; X_{\alpha\text{CoSn}_3} = 0.75; X_{(\beta\text{Sn})} = 1$	Eutectic (E2) ^{C, D}	~502 ~501 502 505 502 504	[7] [8] [23] ^E [25] ^E [26] ^E this work
$\beta\text{Sn} \leftrightarrow \alpha\text{Sn}$ $X_{\beta\text{Sn}} = 1; X_{\alpha\text{Sn}} = 1$ $\alpha\text{CoSn}_3 + \beta\text{Sn} \leftrightarrow \alpha\text{Sn}$ $X_{\alpha\text{CoSn}_3} = 0.75; X_{\beta\text{Sn}} = 1; X_{\alpha\text{Sn}} = 1$	Allotropic transformation and related invariant (PD3) ^C	286 286	[15, 16] ^E this work

^A – recalculated temperatures (normalized to the contemporary accepted value of the cobalt melting point);

^B – equilibrium related with order-disorder transformation and nearly degenerated;

^C – degenerated three-phase equilibrium (the compositions of two coexisting phases are very close one to another);

^D – the melting point of pure Sn is 505.08 K;

^E – assessed values

The intermediate phases denoted as β (βCoSn_3 , $\beta\text{Co}_3\text{Sn}_2$) are high-temperature forms, corresponding to the pertinent α phases (i.e. those stable at room-temperature). C ö m e r t and P r a t t [12, 14] determined Co_3Sn_2 homogeneity range (approx. 40 to 42 at. % Sn) using a variety of techniques (electromotive force measurements, X-rays, metallographic and thermo-analytical methods). They have revealed that the temperature of the transformation $\beta\text{Co}_3\text{Sn}_2 \leftrightarrow \alpha\text{Co}_3\text{Sn}_2$ has the value of $567 \pm 17^\circ\text{C}$ (or 840 ± 17 K, Table 2) on the Co-rich side of the compound.

All intermediate phases melt peritectically (Table 2) except $\beta\text{Co}_3\text{Sn}_2$ that melts congruently at around 1200°C [14]. In the present work, the latter value has been retained, while in some previous assessments [15, 23] the temperature of 1170°C is accepted. J i a n g et al. [25] and L i u et al. [26] accept this value (1200°C) as well. The calculated congruent melting temperature of $\beta\text{Co}_3\text{Sn}_2$ is 1181°C [25] and 1199°C [26].

We have to note that L i u et al. [26] ignored the existence of the CoSn_3 phase and have modeled both Co_3Sn_2 modifications as stoichiometric phases. Moreover, these authors seemed to be unaware about the liquid

phase enthalpy values obtained by L ü c k et al. [19]. That is why the assessment of L i u et al. [26] seems not suitable for further comparison with the results of the present work.

Another difference between the input data used in this study and those of J i a n g et al. [25] is that tin activities (a_{Sn}) measured by E r e m e n k o et al. [22] at 1573 K in liquid Co-Sn alloys, by the effusion method, have not been fully accepted here by reasons discussed below.

The technique used by E r e m e n k o et al. [22] is related to the ratio between the evaporation rates of the pure liquid Sn (v_{Sn}^0) and that (v_{Sn}) of the alloyed liquid phase.

$$a_{\text{Sn}} = v_{\text{Sn}} / v_{\text{Sn}}^0 = p_{\text{Sn}} / p_{\text{Sn}}^0 \quad (2)$$

where p_{Sn} and p_{Sn}^0 are tin partial pressures of the alloys and the pure tin liquid, in the same order.

Thus, the method implies the admission that only monoatomic species of Sn and of Co exist in the liquid phase. The appearance of more kinds of species in the binary melt (e.g. associates Co_3Sn_2) would make invalid

eqn. 1, because the dependence between v_{Sn} and p_{Sn} would be no more correct.

The existence of such species in Co-Sn [38] and Ni-Sn liquid phases [39] has already been discussed. The formation of a metastable Co_3Sn phase, by fast cooling of binary melt, observed by Schluckebier et al. [11] also illustrates the aptitude of cobalt-tin melts to form associates.

Moreover, short-range ordering is observed in amorphous Co-Sn alloys by Nabil et al. [40]. In addition, Mudry et al. [41] reported X-ray investigations of liquid Co-Sn alloys confirming the tendency to form complexes or associates in the liquid state identified by Komarnitsky et al. [42].

Associates corresponding to the formula Co_2Sn (there is not such an equilibrium phase) have been observed by us during current drop calorimetry studies of the Co-Sn system. The nominal chemical composition of the liquid alloys is 48 at. % Sn. This is experimental indication about the existence of associates in liquid cobalt-tin alloys.

Partial molar dissolution enthalpies in infinitely dilute tin melts and CoSn formation enthalpy have been determined by Torgersen et al. [21] using drop calorimetry. These authors also suggest existence of Co_nSn_m clusters in order to explain their results.

Thus, the results reported by Eremenko et al. seem to be subject of some systematic experimental uncertainties and have not been retained as input data.

Körber and Oelsen [18] were the first to study (at 1773 K only) the mixing enthalpy of the binary melts (Table 1). They reported positive values for tin-rich alloys and negative – for cobalt-rich. Relatively recent experiments by Lück et al. [19] in the temperature interval from 1671 K to 1823 K have not confirmed this data. However, it has become clear that the sign of the enthalpy of mixing changes as function of the temperature (positive – above 1670 K and negative – below this temperature). The results of Lück et al. [19] have been selected for this work, while those of Körber and Oelsen [18] have not been used.

Tin activities in solid cobalt-tin phases have been measured at three temperatures by Cömert and Pratt [12] by means of the electromotive force method (Table 2).

Experimental data for the enthalpies of formation of βCo_3Sn_2 and CoSn have been obtained by Predel and Vogelbein [20].

The lattice stabilities of the pure elements and the optimised coefficients obtained in this work are presented in Table 3.

TABLE 3

Thermodynamic database file for calculation of the Co-Sn phase diagram

Functions describing the contributions of the various configurations of the phase Co_3Sn_2

Contribution of the configuration Co:Co (on the third and the fourth sublattices)

FUNCTION GREFCOCO = -20739.5

Contribution of the configuration Va:Va (on the third and the fourth sublattices)

FUNCTION GREFVAVA = -35292.4+11.5636*T

Interaction parameter of zero degree of the configuration Co:Va (on the third and the fourth sublattices) in disordered state

FUNCTION L0COVADI = -34491.7

Contribution of the configuration Co:Va (on the third and the fourth sublattices) in ordered state

FUNCTION G0COVAOR = -10100+7.6252*T

Interaction parameter of first degree of the configuration Co:Va (on the third and the fourth sublattices) in disordered state

FUNCTION L1COVADI = -9313.2

Interaction parameter of first degree of the configuration Co:Va (on the third and the fourth sublattices) in ordered state

FUNCTION L1COVACO = 3471

TABLE 3. (continuation)

Description of the Gibbs energies of the binary Co-Sn phases
<p>PHASE ACOSN3 (αCOSN₃) 2 SUBLATTICES, SITES .25: .75 CONSTITUENTS: CO : SN</p> <p>$G(\text{ACOSN3,CO:SN;0}) - 0.25 \text{H298}(\text{HCP_A3,CO;0}) - 0.75 \text{H298}(\text{BCT_A5,SN;0}) =$ $-11875 + 2.5 * T + .25 * \text{GHSERCO} + .75 * \text{GHSERSN}$</p>
<p>PHASE BCT.A5 (βSN) CONSTITUENTS: SN</p> <p>$G(\text{BCT_A5,SN;0}) - \text{H298}(\text{BCT_A5,SN;0}) = 100.00 < T < 3000: + \text{GHSERSN}$</p> <p>Note: first arrangement is Co:Sn:Co,Va:Co,Va; second (ordered) is: Co:Sn:Co:Va;</p>
<p>PHASE CO3SN2 EXCESS MODEL IS REDLICH-KISTER_MUGGIANU 4 SUBLATTICES, SITES 1: 1: .5: .5 CONSTITUENTS: CO : SN : CO,VA : CO,VA</p> <p>$G(\text{CO3SN2,CO:SN:CO:CO;0}) - 2 * \text{H298}(\text{HCP_A3,CO;0}) - \text{H298}(\text{BCT_A5,SN;0}) = + \text{GREFCOCO} + 2 * \text{GHSERCO} + \text{GHSERSN}$ $G(\text{CO3SN2,CO:SN:VA:CO;0}) - 1.5 * \text{H298}(\text{HCP_A3,CO;0}) - \text{H298}(\text{BCT_A5,SN;0}) =$ $+ \text{G0COVAOR} + .5 * \text{GREFCOCO} + .5 * \text{GREFVAVA} + .25 * \text{L0COVADI} + 1.5 * \text{GHSERCO} + \text{GHSERSN}$ $G(\text{CO3SN2,CO:SN:CO:VA;0}) - 1.5 * \text{H298}(\text{HCP_A3,CO;0}) - \text{H298}(\text{BCT_A5,SN;0}) =$ $+ \text{G0COVAOR} + .5 * \text{GREFCOCO} + .5 * \text{GREFVAVA} + .25 * \text{L0COVADI} + 1.5 * \text{GHSERCO} + \text{GHSERSN}$ $G(\text{CO3SN2,CO:SN:VA:VA;0}) - \text{H298}(\text{HCP_A3,CO;0}) - \text{H298}(\text{BCT_A5,SN;0}) =$ $+ \text{GREFVAVA} + \text{GHSERCO} + \text{GHSERSN}$ $L(\text{CO3SN2,CO:SN:CO,VA:CO;0}) = +.25 * \text{L0COVADI} + .375 * \text{L1COVADI} - \text{G0COVAOR} - \text{L1COVACO}$ $L(\text{CO3SN2,CO:SN:CO,VA:CO;1}) = +.125 * \text{L1COVADI} + \text{L1COVACO}$ $L(\text{CO3SN2,CO:SN:CO:CO,VA;0}) = +.25 * \text{L0COVADI} + .375 * \text{L1COVADI} - \text{G0COVAOR} - \text{L1COVACO}$ $L(\text{CO3SN2,CO:SN:CO:CO,VA;1}) = +.125 * \text{L1COVADI} + \text{L1COVACO}$ $L(\text{CO3SN2,CO:SN:VA:CO,VA;0}) = +.25 * \text{L0COVADI} - .375 * \text{L1COVADI} - \text{G0COVAOR} + \text{L1COVACO}$ $L(\text{CO3SN2,CO:SN:VA:CO,VA;1}) = +.125 * \text{L1COVADI} + \text{L1COVACO}$ $L(\text{CO3SN2,CO:SN:CO,VA:VA;0}) = +.25 * \text{L0COVADI} - .375 * \text{L1COVADI} - \text{G0COVAOR} + \text{L1COVACO}$ $L(\text{CO3SN2,CO:SN:CO,VA:VA;1}) = +.125 * \text{L1COVADI} + \text{L1COVACO}$</p>
<p>PHASE COSN 2 SUBLATTICES, SITES .5: .5 CONSTITUENTS: CO : SN</p> <p>$G(\text{COSN,CO:SN;0}) - 0.5 * \text{H298}(\text{HCP_A3,CO;0}) - 0.5 * \text{H298}(\text{BCT_A5,SN;0}) =$ $-21200 + 5.223 * T + .5 * \text{GHSERCO} + .5 * \text{GHSERSN}$</p>
<p>PHASE COSN2 2 SUBLATTICES, SITES .3333: .6667 CONSTITUENTS: CO : SN</p> <p>$G(\text{COSN2,CO:SN;0}) - 0.3333 * \text{H298}(\text{HCP_A3,CO;0}) - 0.6667 * \text{H298}(\text{BCT_A5,SN;0}) =$ $-15170 + 2.741 * T + .3333 * \text{GHSERCO} + .6667 * \text{GHSERSN}$</p>

TABLE 3. (continuation)

<p>PHASE COSN3 (βCOSN₃) 2 SUBLATTICES, SITES .25: .75 CONSTITUENTS: CO : SN</p> <p>$G(\text{COSN3,CO:SN;0}) - 0.25 \text{ H298}(\text{HCP_A3,CO;0}) - 0.75 \text{ H298}(\text{BCT_A5,SN;0}) = -10505 + .25 * \text{GHSERCO} + .75 * \text{GHSERSN}$</p> <p>PHASE DIAMOND_A4 (αSN) CONSTITUENTS: SN</p> <p>$G(\text{DIAMOND_A4,SN;0}) - \text{H298}(\text{BCT_A5,SN;0}) =$ $100.00 < T < 298.14: -9579.608 + 113.992361 * T - 22.972 * T * \text{LN}(T)$ $- .00813975 * T^{**2} + 2.7288E-06 * T^{**3} + 25615 * T^{**}(-1)$ $298.14 < T < 800.00: -9063.001 + 104.831115 * T - 21.5750771 * T * \text{LN}(T)$ $- .008575282 * T^{**2} + 1.784447E-06 * T^{**3} - 2544 * T^{**}(-1)$ $800.00 < T < 3000.00: -10909.351 + 147.381111 * T - 28.4512 * T * \text{LN}(T)$</p> <p>PHASE FCC_A1 EXCESS MODEL IS REDLICH-KISTER_MUGGIANU ADDITIONAL CONTRIBUTION FROM MAGNETIC ORDERING Magnetic function below Curie Temperature $+1 - .860338755 * \text{TAO}^{**}(-1) - .17449124 * \text{TAO}^{**3} - .00775516624 * \text{TAO}^{**9}$ $- .0017449124 * \text{TAO}^{**15}$ Magnetic function above Curie Temperature $- .0426902268 * \text{TAO}^{**}(-5) - .0013552453 * \text{TAO}^{**}(-15) - 2.84601512E-04 * \text{TAO}^{**}(-25)$</p> <p>2 SUBLATTICES, SITES 1: 1 CONSTITUENTS: CO,SN : VA</p> <p>$G(\text{FCC_A1,CO:VA;0}) - \text{H298}(\text{HCP_A3,CO;0}) = +\text{GCOFCC}$ $\text{TC}(\text{FCC_A1,CO:VA;0}) = 1396$ $\text{BMAGN}(\text{FCC_A1,CO:VA;0}) = 1.35$ $G(\text{FCC_A1,SN:VA;0}) - \text{H298}(\text{BCT_A5,SN;0}) = 298.14 < T < 3000.00: +5510 - 8.46 * T + \text{GHSERSN}$ $\text{TC}(\text{FCC_A1,CO,SN:VA;0}) = -1720$ $\text{L}(\text{FCC_A1,CO,SN:VA;0}) = -19000 + 24.672 * T$</p> <p>PHASE HCP_A3 EXCESS MODEL IS REDLICH-KISTER_MUGGIANU ADDITIONAL CONTRIBUTION FROM MAGNETIC ORDERING Magnetic function below Curie Temperature $+1 - .860338755 * \text{TAO}^{**}(-1) - .17449124 * \text{TAO}^{**3} - .00775516624 * \text{TAO}^{**9}$ $- .0017449124 * \text{TAO}^{**15}$ Magnetic function above Curie Temperature $- .0426902268 * \text{TAO}^{**}(-5) - .0013552453 * \text{TAO}^{**}(-15) - 2.84601512E-04 * \text{TAO}^{**}(-25)$</p> <p>2 SUBLATTICES, SITES 1: .5 CONSTITUENTS: CO,SN : VA</p> <p>$G(\text{HCP_A3,CO:VA;0}) - \text{H298}(\text{HCP_A3,CO;0}) = +\text{GHSERCO}$ $\text{TC}(\text{HCP_A3,CO:VA;0}) = 1396$ $\text{BMAGN}(\text{HCP_A3,CO:VA;0}) = 1.35$ $G(\text{HCP_A3,SN:VA;0}) - \text{H298}(\text{BCT_A5,SN;0}) = +\text{GSNHCP}$ $\text{TC}(\text{HCP_A3,CO,SN:VA;0}) = -1720$ $\text{L}(\text{HCP_A3,CO,SN:VA;0}) = +9000$</p>
--

TABLE 3. (continuation)

<p>PHASE LIQUID</p> <p>EXCESS MODEL IS REDLICH-KISTER_MUGGIANU</p> <p>CONSTITUENTS: CO,SN</p> <p>$G(\text{LIQUID,CO;0})-H298(\text{HCP_A3,CO;0}) = 298.14 < T < 1768.00: +15085.037 - 8.931932 * T - 2.19801E-21 * T^{**7} + \text{GHSERCO}$</p> <p>$1768.00 < T < 6000.00: +16351.056 - 9.683796 * T - 9.3488E+30 * T^{**(-9)} + \text{GHSERCO}$</p> <p>$G(\text{LIQUID,SN;0})-H298(\text{BCT_A5,SN;0}) = 100.00 < T < 3000.00: +\text{GSNLIQ}$</p> <p>$L(\text{LIQUID,CO,SN;0}) = -113890 + 568.4038 * T - 68.169 * T * \text{LN}(T)$</p> <p>$L(\text{LIQUID,CO,SN;1}) = -56193.26 + 283.7657 * T - 33.6875 * T * \text{LN}(T)$</p>
--

In Fig. 2 experimental [20, 21] and calculated in this work integral molar enthalpies of formation (ΔH^F) of the solid Co-Sn phases are represented, showing good agreement between both kinds of values. The ΔH^F values, estimated by C ö m e r t and P r a t t [14], on the basis of electromotive-force measurements, are plotted too. The latter authors have assessed the entropies of the Co-Sn compounds as well (Table 5 of ref. [14]), thus we were able to calculate the relevant molar G i b b s energies of formation at 298.15 K. We found that Co_3Sn_2 G i b b s energy of formation, estimated according to these data, is not large (negative) enough to keep it stable at 298.15 K. Thus, care has been taken during the optimisation to assure the stability of this phase relatively to the adjacent (ϵCo) and CoSn . That is why, as one can see in Figs. 3A,B the optimised values of Sn partial chemical potentials in Co_3Sn_2 are larger (by absolute value) than these found by C ö m e r t and P r a t t [14], while calculated and measured chemical potentials of tin, in the other phases (including the liquid) are in good agreement.

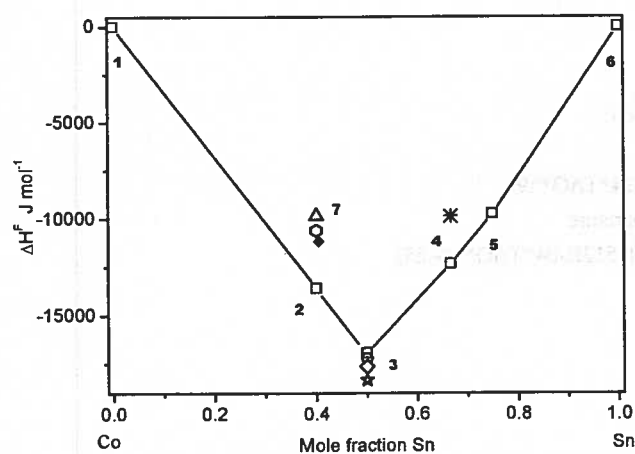


Fig. 2. Integral molar enthalpies of formation at 298.15 K (ΔH^F kJ.mol^{-1}) of cobalt-tin alloys calculated in this work (1 - HCP Co; 2 - $\alpha\text{Co}_3\text{Sn}_2$; 3 - CoSn ; 4 - CoSn_2 ; 5 - αCoSn_3 ; 6 - (βSn); 7 - $\beta\text{Co}_3\text{Sn}_2$) compared with experimental values of P r e d e l and V o g e l b e i n [20] (\circ) and of T o r g e r s e n e t a l. [21] (\diamond). Calculated and experimental [20] values for $\beta\text{Co}_3\text{Sn}_2$ at 1083 K are symbolised

by Δ and \ominus , respectively. The enthalpies of formation derived by C ö m e r t and P r a t t [12] are represented by the symbols: \blacklozenge , \star and $*$. Mole fractions of tin are plotted along the abscissa. Reference states are HCP Co and (βSn) at 298.15 K

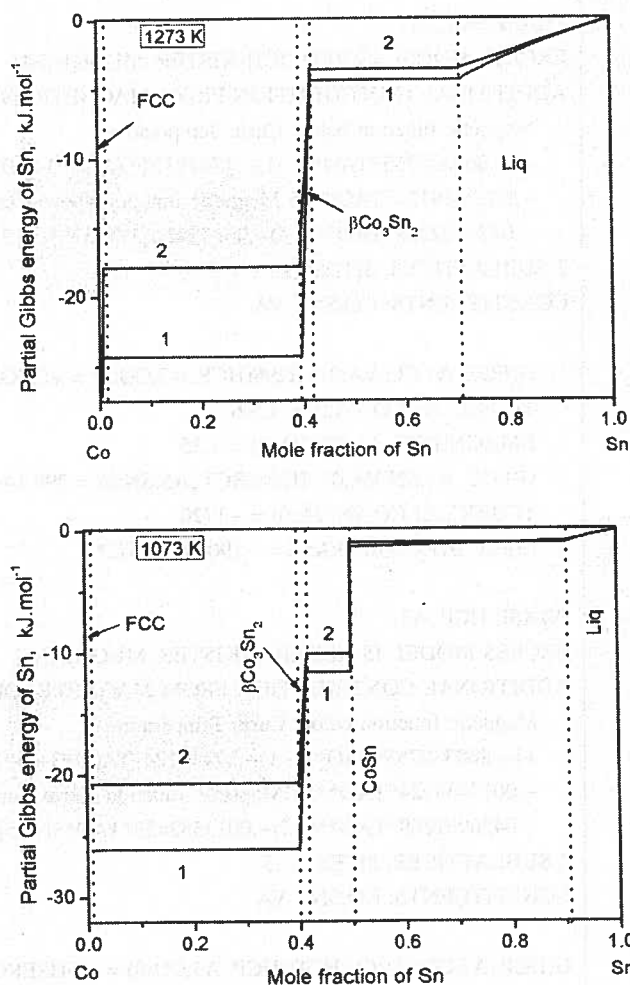


Fig. 3. Calculated (line 1) and measured (line 2) by C ö m e r t and P r a t t [6] partial Gibbs energies of tin at 1273 K (3A) and at 1073 K (3B). Reference state is liquid Sn at the corresponding temperatures

In Fig. 4 the calculated and experimental [19] integral molar enthalpies of formation (ΔH^F) of the liquid

phase are juxtaposed. Sign-variable temperature dependence of the integral molar enthalpies of formation is observed (the ΔH^F values at 1573 K are added in order to illustrate the change of the sign). The calculated values are in good agreement with the experimental ones taking into account possible scattering of the calorimetric values.

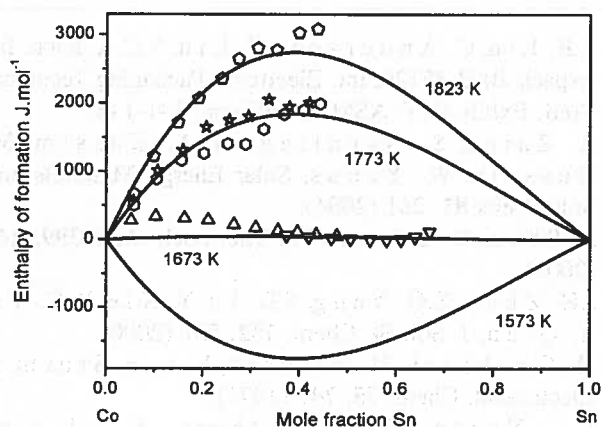


Fig. 4. Integral molar enthalpies of formation (ΔH^F kJ.mol⁻¹) of the liquid cobalt-tin solutions at 1873 K, 1773 K, 1673 K and 1573 K (solid lines) compared with experimental data of Lück et al. [13]: \ominus – 1873 K; \star – 1780 K; \circ – 1759 K; \triangle – 1675; ∇ – 1671 K. Reference states are liquid Co and Sn at the respective temperatures

According to some liquid phase thermochemical data [18, 22] strong concentration dependence of the sign of deviation from ideal behavior exists. Such deviations have not been reproduced, because priority has been given to the data of Lück et al. [19]. It is of worth noting that the extremum on the curve, representing the concentration dependence of the liquid solutions enthalpies of formation, coincides with the composition of the congruently melting phase $\beta\text{Co}_3\text{Sn}_2$ as expected from theoretical considerations.

Other experimental and assessed quantities that can be compared are the partial molar dissolution enthalpies of cobalt in infinitely dilute tin melts, determined by Torgersen et al. [21] at 874 K (12 kJ.mol⁻¹) and 1173 K (32 kJ.mol⁻¹). The corresponding values obtained in this work (12 and 32 kJ.mol⁻¹, respectively) are in excellent agreement with the experimental ones.

The calculated phase diagram (for temperatures above 250 K) is presented in Figs. 5A and 5B. The calculated temperatures of the invariants are juxtaposed with experimental data in Table 2. The most radical difference with some previously accepted variants of the Co-Sn phase diagram [8–10] consists in the admittance that the eutectic invariant E1 is situated at around 15 K higher temperature (i.e. at 1398±2 K). We must concede

that some authors have already adopted the recent value [23, 24]. The experimental data of Lewkonja [7], as normalized in this work, indicate this temperature as well.

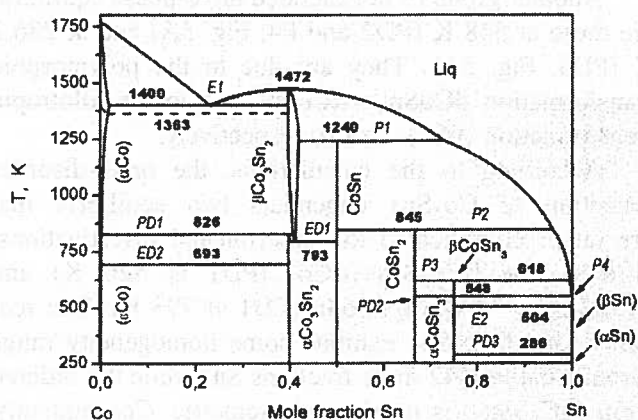


Fig. 5. a) Co-Sn phase diagram calculated in this work. The dashed line represents the Curie temperature

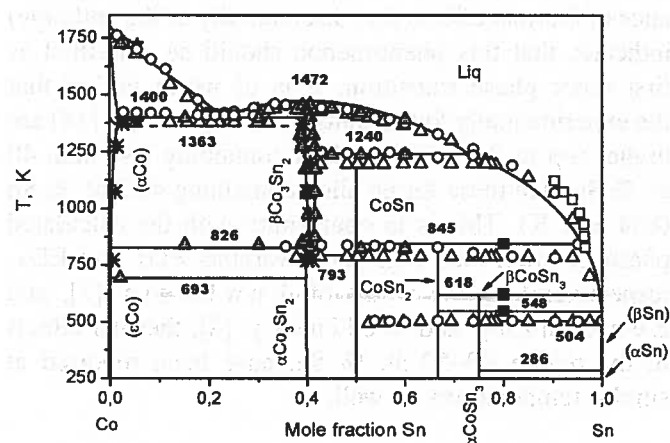


Fig. 5. b) The calculated Co-Sn equilibrium phase diagram with selected topological experimental data: Lewkonja [7] – \circ ; Zemczuzny and Belinsky [8] – \square ; Hashimoto [9] – \star ; Darby and Jugle [10] – \square ; Cömertand Pratt [11] – \triangle ; Cömert and Pratt [14] – \blacktriangle ; Lang and Jeitschko [17] – \blacksquare

We would like to emphasize that, studies concerning the exact compositions of the eutectic and the peritectic points are lacking, and the literature data about them have merely been assessed. That is why, in Tab. 2 are shown calculated concentrations only.

The low-temperature equilibrium E2 could be considered as degenerated one, because the compositions of two coexisting phases (liquid solution and βSn) are practically equal.

The equilibrium $(\alpha\text{Co}) \leftrightarrow (\epsilon\text{Co}) + \alpha\text{Co}_3\text{Sn}_2$ (denoted as ED2 in Table 2) is resolved in this work as (degener-

ated) eutectoid decomposition. Taking into account that the polymorphic transition of the pure cobalt is sluggish (see also [36]) it would be useful but not easy to get reliable experimental information about the characteristics of this equilibrium.

Another group of degenerated three-phase equilibria are these at 548 K (PD2 and P4, Fig. 5A) and at 286.2 K (PD3, Fig. 5A). They are due to the polymorphic transformation $\beta\text{Co}_3\text{Sn}_2 \leftrightarrow \alpha\text{Co}_3\text{Sn}_2$ and to the allotropic transformation (βSn) (αSn), respectively.

According to the calculations, the order-disorder transition of Co_3Sn_2 engenders two equilibria that are rather complicated for experimental investigations: $\alpha\text{Co}_3\text{Sn}_2 \leftrightarrow \beta\text{Co}_3\text{Sn}_2 + (\alpha\text{Co})$ (PD1 at 826 K) and $\beta\text{Co}_3\text{Sn}_2 \leftrightarrow \alpha\text{Co}_3\text{Sn}_2 + \text{CoSn}$ (ED1 at 793 K). The reason is that $\beta\text{Co}_3\text{Sn}_2$ exhibits some homogeneity range (around 0.4 to 0.42 mole fractions Sn) while the ordered form ($\alpha\text{Co}_3\text{Sn}_2$) is nearly stoichiometric. Consequently, the equilibrium compositions of both coexisting modifications are very close one to another.

Experimental data about the temperature of the above mentioned order-disorder transition have been obtained [8] by differential thermal analyses. The appearance of thermal effects (i.e. discontinuity of the enthalpy) indicates that this phenomenon should be classified as first order phase transition. It is of worth noting that the experimentally found transition temperatures [14] are higher (up to 861 K) for alloys containing less than 40 at. % Sn than these for an alloy containing 40.5 at. % Sn (834 \pm 11 K). This is in conformity with the calculated phase diagram (see Fig. 5A, invariants PD1 and ED1, respectively). In the works of Lewkonja [7], and Zemczuzny and Belinsky [8], thermal effects in the region 40–50 at. % Sn, have been reported at similar temperatures as well.

3. Conclusions

The thermochemical information about the binary Co-Sn system seems abundant at a first glance. However, different literature sources contradict one to another and some of them need to be updated with the contemporary value of the melting temperature of pure cobalt. The accuracy of the assessed peritectic points could hardly be estimated due to lack of precise data. Similar concerns are valid for the invariants related with the order-disorder transformation of Co_3Sn_2 .

Nevertheless, the CALPHAD method has been used successfully and coefficients for reasonable description of the phase equilibria and thermodynamic properties of the stable Co-Sn phases have been obtained.

Acknowledgements

This work is related with the European concerted action for development of lead-free solders, COST 531.

REFERENCES

- [1] L.B. Liu, C. Andersson, J. Liu, Y.C. Chan, Interpack 2003-35126, Int. Electronic Packaging Technical Conf. Exhib. (NY: ASME, 2003) pp. 141-146.
- [2] Z. Zaina, S. Nagalingam, A. Kassim, M. Hussein, W. Yunus, Solar Energy Materials and Solar Cells **81**, 261 (2004).
- [3] J. Shen, R. Blachnik, Thermoch. Acta **399**, 245 (2003).
- [4] J.H. Zhan, X.G. Yang, S.D. Li, Y. Xie, W.C. Yu, Y. Qian, J. Sol. St. Chem. **152**, 537 (2000).
- [5] H. Cnobloch, H. Nischik, F. von Sturm, J. Electroanal. Chem. **75**, 747 (1977).
- [6] L. Norén, R.L. Withers, F. Javier García-García, Ann-Kristin Larsson, Solid St. Sciences **4**, 27 (2002).
- [7] K. Lewkonja, Z. Anorg. Allg. Chem. **59**, 294 (1908).
- [8] S.F. Zemczuzny, S.W. Belinsky, Z. Anorg. Allg. Chem. **59**, 364 (1908).
- [9] U. Hashimoto, J. Jpn. Inst. Met. **2**, 67 (1938).
- [10] J.B. Darby, D.B. Juggle, Trans. Metall. Soc. AIME **245** (1969) 2515.
- [11] G. Schluckebier, E. Wachtel, B. Predel, Z. Metallkd. **71**, 456 (1980).
- [12] H. Cömert, J.N. Pratt, Thermochim. Acta **84**, 273 (1985).
- [13] M. Singh, M. Barkei, G. Inden, S. Bhan, Phys. Stat. Sol. (a) **87**, 165 (1985).
- [14] H. Cömert, J.N. Pratt, Metall. Trans. A **23**, 2401 (1992).
- [15] M. Hansen, K. Anderko, Constitution of Binary Alloys, 2nd edn., McGraw-Hill, NY, 1958.
- [16] T. Massalski, CD ROM: Binary Alloy Phase Diagrams, ASM International, OH, USA, 1996.
- [17] A. Lang, W. Jeitschko, Z. Metallkd **87**, 759 (1996).
- [18] F. Körber, W. Oelsen, Mitt. Kaiser-Wilhelm-Inst. Eisenforsch. Dusseldorf **19**, 209 (1937).
- [19] R. Lück, J. Tomiska, B. Predel, Z. Metallkde. **82**, 944 (1991).
- [20] B. Predel, W. Vogelbein, Thermochim. Acta **30**, 201 (1979).
- [21] A. Torgersen, H. Bros, R. Castanet, A. Kjekshus, J. Alloys Comp. **307**, 167 (2000).
- [22] V. Eremenko, G. Lukashenko, V. Pritula, Izv. Akad. Nauk SSSR, Met. **3**, 82 (1971).
- [23] K. Ishida, T. Nishizawa, J. Phase Equilibria **12**, 88 (1991).
- [24] H. Okamoto, J. Phase Equilibria **14**, 3 (1993).

- [25] M. Jiang, J. Sato, I. Ohnuma, R. Kainuma, K. Ishida, CALPHAD (Computer Coupling of Phase Diagrams and Thermochemistry) **28**, 213 (2004).
- [26] L. Liu, C. Andersson, J. Liu, J. Electr. Mater. **33**, 935 (2004).
- [27] A. Dinsdale, A. Watson, A. Kroupa, J. Vrestal, A. Zemanova, J. Vizdal (Eds.), COST 531 Thermodynamic Database for Lead-free Solder Alloys, Version 1.2 (2005). (http://www.slihot.co.uk/COST531/td_database.htm)
- [28] A.T. Dinsdale, CALPHAD **15**, 317 (1991).
- [29] M. Hillert, M. Jarl, CALPHAD **2**, 227 (1978).
- [30] S. Lidin, A.-K. Larsson, J. Sol. State Chem. **118**, 313 (1995).
- [31] A.-K. Larsson, R. Withers, L. Steinberg, J. Sol. State Chem. **127**, 222 (1996).
- [32] A. Leineweber, M. Ellner, E.J. Mittemeijer, J. Sol. State Chem. **159**, 191 (2001).
- [33] P. Waldner, H. Ipsier, Intermetallics **10**, 485 (2002).
- [34] I. Ansara, N. Dupin in: COST 507, Definition of thermochemical and thermophysical properties to provide a database for the development of new light alloys, Vol. 2, 1998, European Commission, Belgium.
- [35] G.P. Vassilev, M. Jiang, J. Phase Equilibria and Diffusion **25** (3), 259 (2004).
- [36] E. Teatum, K. Schneidner, J. Waber, Compilation of calculated data useful in predicting metallurgical behavior of the elements in binary alloy systems, LA-2345, Los Alamos Scientific Laboratory (1960).
- [37] E. Sokolovskaja, L. Guzej, Metallochimia (in Russian), Ed. House of the Moscow University, Moscow, 1986 (see WWW.WEBELEMENTS.COM as well).
- [38] M. Ivanov, Z. Metallkd **82**, 53 (1991).
- [39] M. Hoch, I. Arpshofen, B. Predel, Z. Metallkd **75**, 30 (1984).
- [40] H. Nabil, M. Piecuch, J. Durand, G. Marchall, J. de Physique **46** (C-8), 229 (1985).
- [41] S. Mudry, M. Komarnitsky, A. Korolyshyn, S. Prokhorenko, Proc. 14th Int. Scientific Conf. On Advanced Materials and Technologies, Glivice-Zakopane, Poland, 17-21 May 1995, pp. 333-336.
- [42] M. Komarnitsky, S. Mudry, V. Halchak, JALCOM **242**, 157 (1996).